Proceedings of the
Annual Stability Conference
Structural Stability Research Council
St. Louis, Missouri, April 16-20, 2013

Localized Web Buckling of Double-Coped Beams

Bo Dowswell[1], Robert Whyte[2]

Abstract
In beam-to-girder connections, the beam is usually coped to allow a standard connection to the girder web. If the beam and girder are of equal depth, both flanges must be coped. Due to the flexural and shear stresses in the coped portion of the web, web buckling can limit the local strength. The AISC *Steel Construction Manual* provides a design procedure for web buckling of double-coped beams. However, the equations are not valid if the cope depth exceeds 20% of the beam depth. Although the design equations were developed for beams with equal cope sizes at the top and bottom, it is common for the cope sizes to be unequal. This research addresses three issues related to the local stability of double-coped beams: 1. Cope depths greater than 20% of the beam depth, 2. Unequal cope depths at the top and bottom, 3. Unequal cope lengths at the top and bottom. 54 elastic finite element models were used to determine the effect of each variable on the critical load. A semi-empirical design model, with lateral-torsional buckling as the basis, was used to formulate equations to predict localized web buckling of double-coped beams. A buckling modification factor was determined by curve fitting the finite element data.

1. Introduction

In beam-to-girder connections, the beam is usually coped to allow a standard connection to the girder web. If the beam and girder are of equal depth, both flanges must be coped as shown in Fig. 1. The cope length can be large at skewed beam connections, connections to wide flange truss chords, and other less common framing conditions. Additionally, it is common for double-coped beams to have unequal cope depths at the top and the bottom, and some connections require unequal cope lengths at the top and bottom flange.

Due to the flexural and shear stresses in the coped portion of the web, web buckling can limit the local strength. The AISC *Steel Construction Manual* (AISC, 2011), provides a semi-empirical design procedure for localized stability of double-coped beams. The procedure was developed by Cheng et al. (1984) based on a lateral-torsional buckling model with an adjustment factor determined by curve fitting data from elastic finite element models. Because the adjustment factor was derived empirically, limits of applicability were placed on the design equations. The design procedure is not valid if the cope length exceeds

[1] Principal, ARC International, LLC, <bo@arcstructural.com>
[2] Assistant Project Manager, LBYD, Inc., <rwhyte@lbyd.com>

twice the beam depth or the cope depth exceeds 20% of the beam depth. All of the models had equal cope sizes at both the top and the bottom.

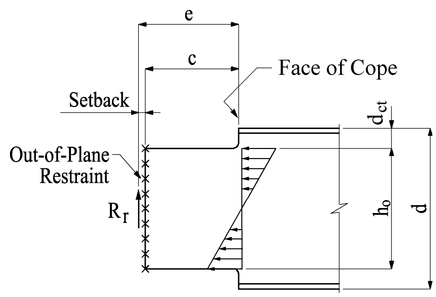

Figure 1. Double-Coped Beam

In many practical cases, the cope geometry falls outside the limits of applicability of the AISC *Manual* procedure. This paper addresses three issues related to the localized web stability of double-coped beams: 1. Cope depths greater than 20% of the beam depth, 2. Unequal cope depths at the top and bottom, 3. Unequal cope lengths at the top and bottom. 54 elastic finite element models were used to determine the effect of each variable on the critical load.

2. Existing Publications

2.1 Cheng et al. (1984)

Cheng et al. (1984) developed the design procedure in the AISC *Steel Construction Manual* (AISC, 2011) with the results of 14 elastic finite element models. BASP finite element software was used as described by Akay et al. (1977). The models were braced laterally at the face of the compression flange cope. The buckled shapes showed that the tension edge of the coped cross section experienced lateral movement and the shear center of the coped region experienced lateral movement and twisting. The semi-empirical design procedure was developed based on a lateral-torsional buckling model with an adjustment factor determined by curve fitting data from the finite element models. All of the models had equal cope sizes at both the top and the bottom.

2.2 Steel Construction Manual (AISC, 2011)

The model for the design procedure developed by Cheng et al. (1984) is shown in Fig. 1. The required flexural strength at the face of the cope is

$$M_r = R_r e \tag{1}$$

The nominal flexural strength is

$$M_n = F_{cr} S_{net} \tag{2}$$

The critical stress is

$$F_{cr} = 0.62\pi E f_d \frac{t_w^2}{c h_0} \le F_y \tag{3}$$

The adjustment factor is

$$f_d = 3.5 - 7.5\left(\frac{d_{ct}}{d}\right) \tag{4}$$

where

E = modulus of elasticity, ksi
F_y = specified minimum yield stress, ksi
R_r = required end reaction, kips
S_{net} = section modulus of the coped section, in.^{3}
c = cope length, in.
d = beam depth, in.
d_{ct} = depth of the top cope, in.
e = distance from the face of the cope to the end reaction, in.
h_o = reduced depth of web, in.
t_w = web thickness, in.

The preceding equations are based on a lateral-torsional buckling model and are valid when $c \le 2d$ and $d_c \le 0.2d$. If $d_c > 0.2d$, the following equations, which are based on a plate buckling model (Muir and Thornton, 2004), are applicable.

$$F_{cr} = F_y Q \tag{5}$$

The reduction factor for plate buckling is

When $\lambda \le 0.7$

$$Q = 1.0 \tag{6a}$$

When $0.7 < \lambda \le 1.41$

$$Q = 1.34 - 0.486\lambda \tag{6b}$$

When $\lambda > 1.41$

$$Q = \frac{1.30}{\lambda^2} \tag{6c}$$

The slenderness parameter is

$$\lambda = \frac{h_0}{10t_w}\sqrt{\frac{F_y}{475 + 280\left(\frac{h_0}{c}\right)^2}} \tag{7}$$

2.3 AISC Specification Section F11

Because the *Manual* equations developed by Cheng et al. (1984) were based on a lateral-torsional buckling model, AISC *Specification* (AISC, 2010) Section F11 will be reviewed here. Section F11 provides design information for the flexural strength and stability of rectangular members bent about their major axis.

For yielding, $\frac{L_b d}{t^2} \le \frac{0.08E}{F_y}$

$$M_n = M_p = F_y Z \le 1.6 M_y \tag{8}$$

For inelastic lateral-torsional buckling, $\frac{0.08E}{F_y} < \frac{L_b d}{t^2} \le \frac{1.9E}{F_y}$

$$M_n = C_b\left[1.52 - 0.274\left(\frac{L_b d}{t^2}\right)\frac{F_y}{E}\right]M_y \le M_p \tag{9}$$

For elastic lateral-torsional buckling, $\frac{L_b d}{t^2} > \frac{1.9E}{F_y}$

$$M_n = F_{cr} S_x \le M_p \tag{10}$$

The critical stress is

$$F_{cr} = \frac{1.9EC_b}{\frac{L_b d}{t^2}} \tag{11}$$

where

C_b = lateral-torsional buckling modification factor
L_b = distance between brace points, in.
M_n = nominal moment, kip-in.
M_y = yield moment, kip-in.
M_p = plastic moment, kip-in.
S_x = elastic section modulus, in.^{3}

Z = plastic modulus, in.^{3}
t = beam width, in.

Eq. 11 is the theoretical solution for lateral-torsional buckling (Timoshenko and Gere, 1961) multiplied by C_b and simplified by substituting the properties for a rectangular cross section. It can be shown that Eq. 3 is equal to Eq. 11 by substituting $t = t_w$, $d = h_0$, $L_b = c$ and $C_b = f_d$ into Eq. 11. Therefore, f_d is simply a lateral-torsional buckling modification factor applied to the theoretical equation for the critical moment of a rectangular beam.

3. Finite Element Models

AISC *Specification* Section F2 equations for lateral-torsional buckling of wide flange beams are based on the theoretical solution (Timoshenko and Gere, 1961), with C_b factors developed primarily using elastic finite element models. The inelastic portion of the buckling curve was developed by mapping, based on limited testing and finite element results in the inelastic zone. Because much of the inelastic research was based on a constant moment along the beam length (C_b = 1), the full beam length was inelastic. Therefore, the buckling curves are conservative for C_b > 1, because they don't account for partial inelasticity along the beam. This same procedure was used in this research to develop equations for the local stability of coped beams.

The finite element program was designed to address three issues related to the local stability of double-coped beams: 1. Cope depths greater than 20% of the beam depth, 2. Unequal cope depths at the top and bottom, 3. Unequal cope lengths at the top and bottom. 54 elastic finite element models were used to determine the effect of each variable on the critical load. Using the variables shown in Fig. 2, the program consisted of 30 models with $c_t = c_b$, 12 models with $c_t > c_b$, and 12 models with $c_t < c_b$. The details are listed in Appendix A Tables A1, A2 and A3, respectively.

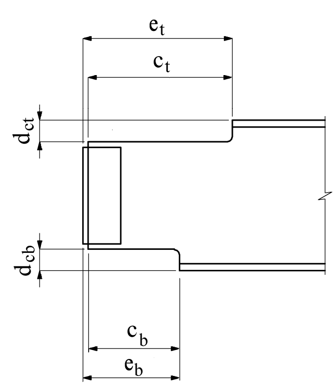

Figure 2. Different Cope Sizes at the Top and Bottom Flanges

All models were built with the nominal dimensions of a W16x26. Following the modeling techniques of Cheng et al. (1984), BASP finite element software was used to determine the critical loads, and the flanges were braced laterally at the face of the cope.

4. Results

All of the finite element models buckled in a similar manner as shown in Fig. 3. Confirming the results of Cheng et al. (1984), the tension edge of the coped cross section experienced lateral translation and the shear center experienced lateral translation and twisting. The compression edge of the coped section buckled in the shape of a half sine wave, which extended partially into the uncoped portion of the beam due to lateral translation at the reentrant corner of the cope.

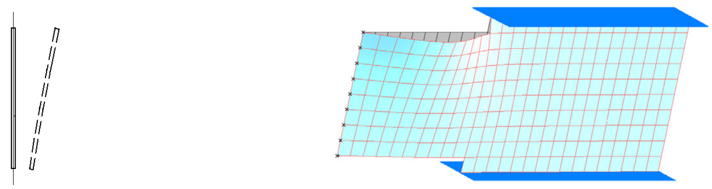

a. $c_t = c_b$

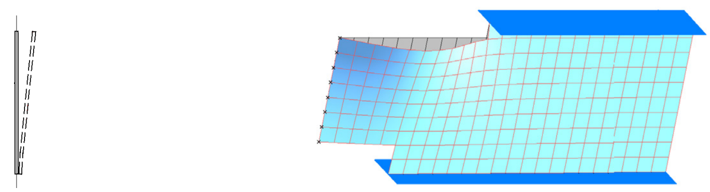

b. $c_t > c_b$

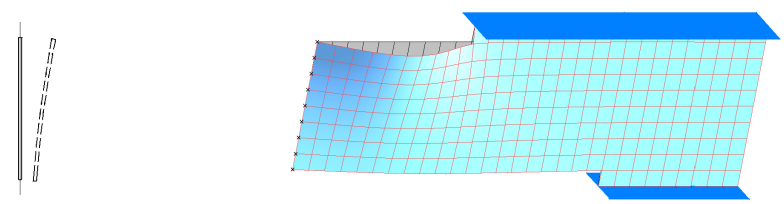

c. $c_t < c_b$

Figure 3. Buckled Shapes

To form a semi-empirical design model, the buckling mode must be identified. The buckled shapes have the appearance of several independent modes, including local buckling, lateral-torsional buckling, shear buckling, and distortional buckling. The dominant buckling mode is dependent on the cope geometry. Short copes are controlled by shear buckling and long copes are controlled by lateral-torsional buckling, with some aspects of local buckling and distortional buckling present in all cope geometries. Because the buckled shapes most closely resemble lateral-torsional buckling over the critical variable range, the design model is based on Eq. 11 with the buckling modification factor, C_b, accounting for contributions from the other buckling modes. C_b was determined by curve fitting the finite element data.

The required flexural strength at the face of the cope is

$$M_r = R_r e_{min} \tag{12}$$

The nominal moment is calculated with Eq. 10 and 11 with $t = t_w$ and $d = h_0$. The equation for C_b is dependent on the c_t/c_b ratio. For beams with $c_t = c_b$, C_b is calculated using Eq. 13 with $L_b = c_t = c_b$. For beams with $c_t < c_b$, C_b is calculated using Eq. 13 with $L_b = 0.9c_t + 0.1c_b$.

$$C_b = \left[3.3 + 0.85\sqrt{\frac{d}{L_b}}\,\mathbf{ln}\left(\frac{L_b}{d}\right)\right]\left[1 - \frac{d_{ct}}{d} + \left(\frac{d_{ct}}{d}\right)^2\right] \tag{13}$$

For beams with $c_t > c_b$, C_b is calculated using Eq. 14 with $L_b = (c_t + c_b)/2$.

$$C_b = \left(\frac{c_b}{c_t}\right)\left[3.3 + 0.85\sqrt{\frac{d}{L_b}}\,\mathbf{ln}\left(\frac{L_b}{d}\right)\right]\left[1 - \frac{d_{ct}}{d} + \left(\frac{d_{ct}}{d}\right)^2\right] \tag{14}$$

where

c_b = length of bottom cope, in.
c_t = length of top cope, in.
d_{cb} = depth of bottom cope, in.
d_{ct} = depth of top cope, in.
e_b = distance from the face of the bottom cope to the end reaction, in.
e_t = distance from the face of the top cope to the end reaction, in.
e_{min} = minimum of e_t and e_b

The results for all models are listed in Tables A1, A2 and A3 in Appendix A. For beams with $c_t = c_b$, the average finite element-to-calculated load ratio is 1.01 and the standard deviation is 0.0535. For $c_t < c_b$, the average load ratio is 1.02 and the standard deviation is 0.0902. For $c_t > c_b$, the average load ratio is 1.06 and the standard deviation is 0.0752.

Eq. 13 is plotted in Fig. 4 and 5 with the finite element results for $c_t = c_b$. Fig. 4 shows C_b versus c_t/d for four values of d_{ct}/d. Fig. 5 shows C_b versus d_{ct}/d for four values of c_t/d.

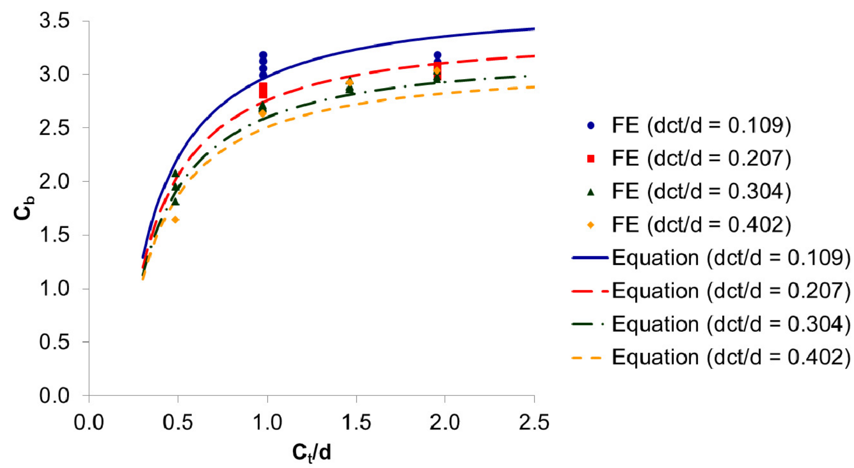

Figure 4. C_b versus c_t/d

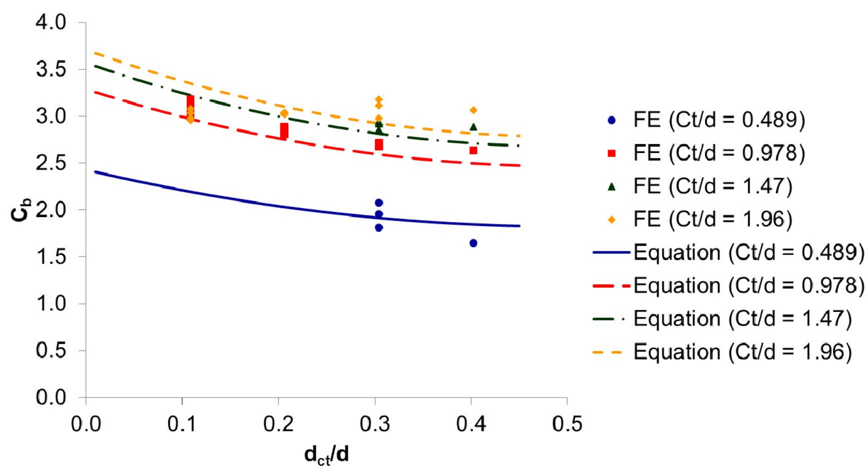

Figure 5. C_b versus d_{ct}/d

5. Design Proposal

To account for inelastic action, AISC *Specification* Section F11 can be used with $t = t_w$ and $d = h_0$. For short cope lengths, the required shear load can be close to the shear yield strength. To account for the interaction between the flexural and shear loads, a reduction factor can be applied to the plastic moment capacity, M_p. Neal (1961) presented Eq. 15 for the plastic capacity of a rectangular member subjected to moment about one axis, axial load, and shear.

$$\frac{M_r}{M_p} + \left(\frac{P_r}{P_y}\right)^2 + \frac{\left(\frac{R_r}{V_n}\right)^4}{1 - \left(\frac{P_r}{P_y}\right)^2} \leq 1.0 \tag{15}$$

where
P_r = required axial load, kips
P_y = axial yield load, kips
R_r = required shear load, kips
V_n = shear yield strength, kips

The plastic moment strength, reduced to account for the required shear load is

$$M_{pv} = M_p \left[1 - \left(\frac{R_r}{V_n}\right)^4\right] \tag{16}$$

The following design procedure is suggested:
For yielding, $\lambda \leq \lambda_p$

$$M_n = M_{pv} \tag{17}$$

For inelastic lateral-torsional buckling, $\lambda_p < \lambda \leq \lambda_r$

$$M_n = C_b \left[1.52 - 0.274\lambda \frac{F_y}{E}\right] M_y \leq M_{pv} \tag{18}$$

For elastic lateral-torsional buckling, $\lambda > \lambda_r$

$$M_n = F_{cr} S_x \leq M_{pv} \tag{19}$$

The critical stress is

$$F_{cr} = \frac{1.9EC_b}{\lambda} \tag{20}$$

where

$$\lambda = \frac{L_b h_0}{t_w^2} \tag{21}$$

$$\lambda_p = \frac{0.08E}{F_y} \tag{22}$$

$$\lambda_r = \frac{1.9E}{F_y} \tag{23}$$

Simplified versions of Eq. 13 and 14 can be used for design purposes. For beams with $c_t = c_b$ and beams with $c_t < c_b$, $L_b = c_t$ and C_b is calculated with Eq. 24.

$$C_b = \left[3 + \mathbf{ln}\left(\frac{L_b}{d}\right)\right]\left(1 - \frac{d_{ct}}{d}\right) \tag{24}$$

For beams with $c_t > c_b$, $L_b = (c_t + c_b)/2$ and C_b is calculated with Eq. 25.

$$C_b = \left(\frac{c_b}{c_t}\right)\left[3 + \mathbf{ln}\left(\frac{L_b}{d}\right)\right]\left(1 - \frac{d_{ct}}{d}\right) \tag{25}$$

The simplified equations are compared to the finite element models in Appendix A Tables A1, A2 and A3. For beams with $c_t = c_b$, the average finite element-to-calculated load ratio is 1.18 and the standard deviation is 0.139. For $c_t < c_b$, the average load ratio is 1.05 and the standard deviation is 0.0736. For $c_t > c_b$, the average load ratio is 1.19 and the standard deviation is 0.0949.

6. Conclusions

This paper addressed three issues related to the localized web stability of double-coped beams: 1. Cope depths greater than 20% of the beam depth, 2. Unequal cope depths at the top and bottom, 3. Unequal cope lengths at the top and bottom. 54 elastic finite element models were used to determine the effect of each variable on the critical load. A semi-empirical design model, with lateral-torsional buckling as the basis, was used to formulate equations to predict localized web buckling of double-coped beams. A buckling modification factor was determined by curve fitting the finite element data.

All of the finite element models buckled in a similar manner, with the tension edge of the coped cross section translating laterally and the shear center of the coped region experiencing lateral translation and twisting. The compression edge of the coped section buckled in the shape of a half sine wave, which extended partially into the uncoped portion of the beam due to lateral translation at the reentrant corner of the cope.

Because the shapes most closely resemble lateral-torsional buckling over the critical variable range, the design model was based on AISC *Specification* Section F11, with the buckling modification factor, C_b, determined by curve fitting the finite element data. For the curve-fit equations, the average finite element-to-calculated load ratio is 1.02 and the standard deviation is 0.0665. The simplified design equations had an average finite element-to-calculated load ratio of 1.15 and a standard deviation of 0.115.

Acknowledgments
Thanks to Professor Joseph Yura at The University of Texas at Austin for providing the finite element program, BASP, used in this study.

Nomenclature

C_b = lateral-torsional buckling modification factor
E = modulus of elasticity, ksi
F_{cr} = critical stress, ksi
F_y = specified minimum yield stress, ksi
L_b = distance between brace points, in.
M_n = nominal moment, kip-in.
M_y = yield moment, kip-in.
M_p = plastic moment, kip-in.
M_{pv} = plastic moment, reduced to account for the required shear load, kip-in.
M_r = required moment, kip-in.
P_r = required axial load, kips
P_y = axial yield load, kips
Q = reduction factor for plate buckling
R_{de} = critical reaction with C_b calculated with the simplified design equation
R_{fe} = critical reaction from finite element model
R_r = required end reaction, kips
R_{re} = critical reaction with C_b calculated with the original regression equation
S_{net} = elastic section modulus of the coped section, in.^{3}
S_x = elastic section modulus, in.^{3}
V_n = shear yield strength, kips
Z = plastic modulus, in.^{3}
c = cope length, in.
c_b = length of bottom cope, in.
c_t = length of top cope, in.
d = beam depth, in.
d_{cb} = depth of bottom cope, in.
d_{ct} = depth of top cope, in.
e = distance from the face of the cope to the end reaction, in.
e_b = distance from the face of the bottom cope to the end reaction, in.
e_t = distance from the face of the top cope to the end reaction, in.
e_{min} = minimum of e_t and e_b
f_d = adjustment factor
h_o = reduced depth of web, in.
t = beam width, in.
t_w = web thickness, in.
λ = slenderness parameter
λ_p = limiting slenderness for the limit state of yielding
λ_r = limiting slenderness for the limit state of inelastic lateral-torsional buckling

References

AISC (2010), *Specification for Structural Steel Buildings*, June 22, American Institute of Steel Construction, Chicago, IL.

AISC (2011), *Steel Construction Manua*l, 14th Edition, American Institute of Steel Construction, Chicago, IL.

Akay, H. U., Johnson, C. P., and Will, K. M. (1977), "Lateral and Local Buckling of Beams and Frames," Journal of the Structural Division, ASCE, Vol. 103, No. ST9, September, pp. 1821-1832.

Cheng, J.J., Yura, J.A., and Johnson, C.P. (1984), "Design and Behavior of Coped Beam," Ferguson Lab Report, The University of Texas at Austin, July.

Muir, L.S. and Thornton, W.A. (2004), "A Direct Method for Obtaining the Plate Buckling Coefficient for Double-Coped Beams," *Engineering Journal*, American Institute of Steel Construction, Third Quarter, Chicago, IL.

Neal, B.G. (1961), "The Effect of Shear and Normal Forces on the Fully Plastic Moment of a Beam of Rectangular Cross Section," Journal of Applied Mechanics, Vol. 28, pp. 269-274.

Timoshenko, S. P. and Gere, J. M. (1961), *Theory of Elastic Stability*, Second Edition, Mcgraw-Hill, New York.

Appendix A. Tables

Table A1. Finite element results with $c_t = c_b$									
Model No.	**c_t in.**	**c_b in.**	**d_{ct} in.**	**d_{cb} in.**	**R_{fe} kips**	**R_{re} kips**	**R_{de} kips**	$\frac{R_{fe}}{R_{re}}$	$\frac{R_{fe}}{R_{de}}$
1	15.4	15.4	1.71	1.71	24.4	22.7	20.3	1.07	1.20
2	15.4	15.4	3.24	1.71	19.3	18.4	15.8	1.05	1.22
3	15.4	15.4	4.78	1.71	15.6	14.9	11.9	1.05	1.31
4	15.4	15.4	6.31	1.71	12.6	11.9	8.53	1.06	1.48
5	15.4	15.4	1.71	3.24	20.9	19.9	17.8	1.05	1.18
6	15.4	15.4	3.24	3.24	16.3	15.8	13.6	1.04	1.20
7	15.4	15.4	4.78	3.24	12.9	12.4	9.92	1.04	1.30
8	15.4	15.4	1.71	4.78	17.6	17.0	15.3	1.03	1.15
9	15.4	15.4	3.24	4.78	13.4	13.1	11.3	1.02	1.19
10	15.4	15.4	1.71	6.31	14.3	14.2	12.7	1.01	1.13
11	30.7	30.7	1.71	1.71	6.09	6.42	6.27	0.948	0.970
12	30.7	30.7	3.24	1.71	5.16	5.20	4.88	0.992	1.06
13	30.7	30.7	4.78	1.71	4.36	4.20	3.67	1.04	1.19
14	30.7	30.7	6.31	1.71	3.63	3.37	2.63	1.08	1.38
15	30.7	30.7	1.71	3.24	5.22	5.62	5.49	0.930	0.951
16	30.7	30.7	3.24	3.24	4.34	4.46	4.19	0.973	1.04
17	30.7	30.7	4.78	3.24	3.57	3.50	3.06	1.02	1.17
18	30.7	30.7	1.71	4.78	4.41	4.81	4.70	0.915	0.937
19	30.7	30.7	3.24	4.78	3.57	3.71	3.49	0.961	1.02
20	30.7	30.7	1.71	6.31	3.63	4.01	3.92	0.906	0.927
21	7.68	7.68	4.78	1.71	41.6	44.1	36.6	0.945	1.14
22	7.68	7.68	6.31	1.71	31.5	35.4	26.2	0.891	1.20
23	7.68	7.68	4.78	3.24	37.4	36.7	30.5	1.02	1.23
24	23.0	23.0	4.78	1.71	7.51	7.19	6.01	1.04	1.25
25	23.0	23.0	6.31	1.71	6.22	5.77	4.31	1.08	1.44
26	23.0	23.0	4.78	3.24	6.15	5.99	5.01	1.03	1.23
27	7.68	7.68	4.78	4.78	31.8	29.4	24.4	1.08	1.31
28	15.4	15.4	4.78	4.78	10.3	9.91	7.94	1.04	1.29
29	23.0	23.0	4.78	4.78	4.87	4.79	4.01	1.02	1.21
30	30.7	30.7	4.78	4.78	2.83	2.80	2.45	1.01	1.16
							Average	1.01	1.18
							Std. Deviation	0.0535	0.139

R_{fe} = critical reaction from finite element model
R_{re} = critical reaction with C_b calculated with the original regression equation
R_{de} = critical reaction with C_b calculated with the simplified design equation

Table A2. Finite element results with $c_t > c_b$									
Model No.	c_t **in.**	c_b **in.**	d_{ct} **in.**	d_{cb} **in.**	R_{fe} **kips**	R_{re} **kips**	R_{de} **kips**	$\frac{R_{fe}}{R_{re}}$	$\frac{R_{fe}}{R_{de}}$
32	30.7	15.4	3.24	3.24	6.87	5.72	5.14	1.20	1.33
34	30.7	15.4	1.71	1.71	8.27	8.24	7.71	1.00	1.07
36	30.7	15.4	1.71	3.24	7.69	7.21	6.74	1.07	1.14
38	30.7	15.4	3.24	1.71	7.41	6.67	6.00	1.11	1.23
40	15.4	7.68	3.24	3.24	20.5	19.2	16.4	1.07	1.25
42	15.4	7.68	1.71	1.71	27.9	27.6	24.5	1.01	1.14
44	15.4	7.68	1.71	3.24	25.7	24.2	21.4	1.06	1.20
46	15.4	7.68	3.24	1.71	22.3	22.4	19.1	0.995	1.17
48	30.7	7.68	3.24	3.24	7.94	6.64	5.84	1.19	1.36
50	30.7	7.68	1.71	1.71	9.10	9.57	8.75	0.952	1.04
52	30.7	7.68	1.71	3.24	8.79	8.37	7.65	1.05	1.15
54	30.7	7.68	3.24	1.71	8.25	7.75	6.81	1.06	1.21
						Average		1.06	1.19
						Std. Deviation		0.0752	0.0949

R_{fe} = critical reaction from finite element model
R_{re} = critical reaction with C_b calculated with the original regression equation
R_{de} = critical reaction with C_b calculated with the simplified design equation

Table A3. Finite element results with $c_t < c_b$									
Model No.	c_t **in.**	c_b **in.**	d_{ct} **in.**	d_{cb} **in.**	R_{fe} **kips**	R_{re} **kips**	R_{de} **kips**	$\frac{R_{fe}}{R_{re}}$	$\frac{R_{fe}}{R_{de}}$
31	15.4	30.7	3.24	3.24	14.1	14.7	13.6	0.959	1.04
33	15.4	30.7	1.71	1.71	21.3	21.1	20.3	1.01	1.05
35	15.4	30.7	1.71	3.24	18.5	18.5	17.8	1.00	1.04
37	15.4	30.7	3.24	1.71	16.5	17.1	15.8	0.962	1.04
39	7.68	15.4	3.24	3.24	42.8	45.1	41.7	0.948	1.03
41	7.68	15.4	1.71	1.71	72.6	65.0	62.4	1.12	1.16
43	7.68	15.4	1.71	3.24	64.4	56.9	54.6	1.13	1.18
45	7.68	15.4	3.24	1.71	48.7	52.6	48.6	0.926	1.00
47	7.68	30.7	3.24	3.24	40.3	41.7	41.7	0.967	0.967
49	7.68	30.7	1.71	1.71	68.3	60.0	62.4	1.14	1.09
51	7.68	30.7	1.71	3.24	61.3	52.5	54.6	1.17	1.12
53	7.68	30.7	3.24	1.71	45.5	48.6	48.6	0.936	0.936
						Average		1.02	1.05
						Std. Deviation		0.0902	0.0736

R_{fe} = critical reaction from finite element model
R_{re} = critical reaction with C_b calculated with the original regression equation
R_{de} = critical reaction with C_b calculated with the simplified design equation